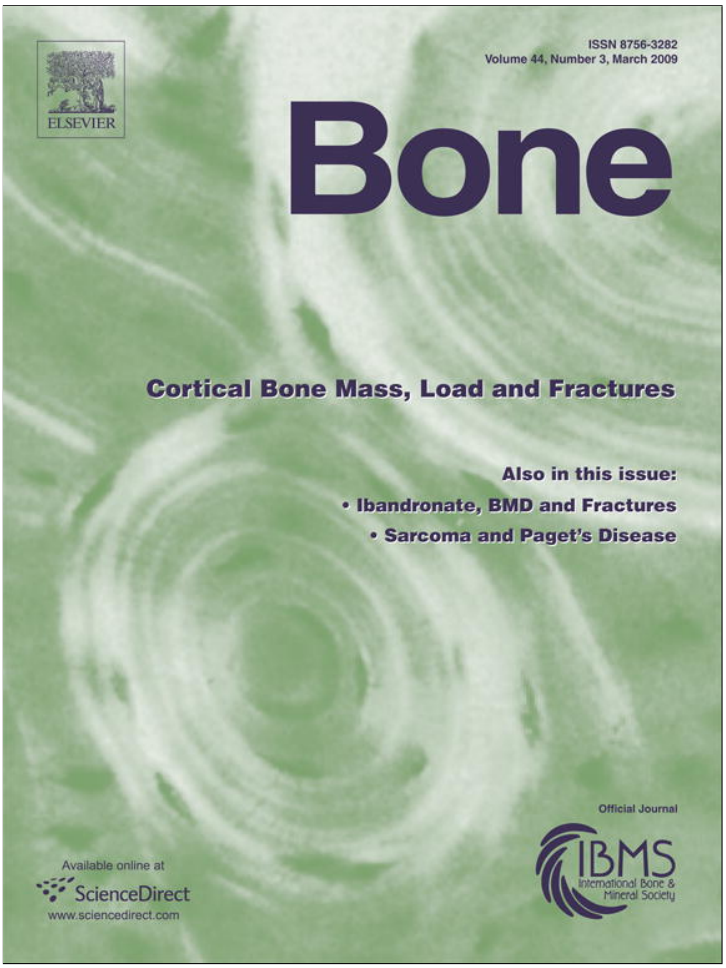

Bone 44 (2009) 392–403

Contents lists available at ScienceDirect

Bone

journal homepage: www.elsevier.com/locate/bone

Interpreting cortical bone adaptation and load history by quantifying osteon morphotypes in circularly polarized light images ☆

John G. Skedros [a,*], Shaun D. Mendenhall [a], Casey J. Kiser [a], Howard Winet [b]

[a] Bone and Joint Research Laboratory, Department of Veterans Affairs Medical Center, The University of Utah Department of Orthopaedic Surgery, Salt Lake City, Utah, USA
[b] University of California, Los Angeles (UCLA) Department of Orthopaedic Surgery, USA

ARTICLE INFO

Article history:
Received 26 June 2008
Revised 23 September 2008
Accepted 30 October 2008
Available online 12 November 2008

Edited by: D. Burr

Keywords:
Osteon
Bone remodeling
Collagen fiber orientation
Bone adaptation
Toughness
Strain mode

ABSTRACT

Birefringence variations in circularly polarized light (CPL) images of thin plane-parallel sections of cortical bone can be used to quantify regional differences in predominant collagen fiber orientation (CFO). Using CPL images of equine third metacarpals (MC3s), R.B. Martin, V.A. Gibson, S.M. Stover, J.C. Gibeling, and L.V. Griffin. (40) described six secondary osteon variants ('morphotypes') and suggested that differences in their regional prevalence affect fatigue resistance and toughness. They devised a numerical osteon morphotype score (MTS) for quantifying regional differences in osteon morphotypes. We have observed that a modification of this score could significantly improve its use for interpreting load history. We hypothesized that our modified osteon MTS would more accurately reveal differences in osteon MTSs between opposing "tension" and "compression" cortices of diaphyses of habitually bent bones. This was tested using CPL images in transverse sections of calcanei from sheep, deer, and horses, and radii from sheep and horses. Equine MC3s and sheep tibiae were examined as controls because they experience comparatively greater load complexity that, because of increased prevalence of torsion/shear, would not require regional mechanical enhancements provided by different osteon morphotypes. Predominant CFO, which can reliably reflect adaptation for a regionally prevalent strain mode, was quantified as mean gray levels from birefringence of entire images (excluding pore spaces) in anterior, posterior, medial, and lateral cortices. Results showed that, in contrast to the original scoring scheme of Martin et al., the modified scheme revealed significant anterior/posterior differences in osteon MTSs in nearly all "tension/compression" bones ($p<0.0001$), but not in equine MC3s ($p=0.30$) and sheep tibiae ($p=0.35$). Among habitually bent bones, sheep radii were the exception; relatively lower osteon populations and the birefringence of the primary bone contributed to this result. Correlations between osteon MTSs using the scoring scheme of Martin et al. with CFO data from all regions of each bone invariably demonstrated weak-to-moderate *negative* correlations. This contrasts with typically high *positive* correlations between modified osteon MTSs and regional CFO. These results show that the modified osteon MTS can be a strong correlate of predominant CFO and of the non-uniform strain distribution produced by habitual bending.

Published by Elsevier Inc.

Introduction

An important concept in bone mechanics is that secondary osteons influence mechanical properties in several ways, including contributing to toughness and fatigue strength by debonding from the interstitial matrix so as to "bridge" developing microcracks [25,39,44]. In a microscopic study of thin sections of diaphyseal cortices of equine third metacarpals (MC3s) viewed in circularly polarized light (CPL), Martin et al. [40] described six phenotypic variants of the secondary osteons. In order to distinguish differences in predominant collagen fiber orientation (CFO) within and between osteons, their study employed the well established method of quantifying birefringence variations in circularly polarized light (CPL) images of plane-parallel sections of cortical bone [12–14]. In addition to identifying these six variants, or osteon 'morphotypes', Martin et al. [40] introduced a numerical method for scoring regional variations in their distribution. In turn, they argued that this spatial histologic heterogeneity is probably important in producing localized enhancements in fatigue life and toughness across the equine MC3 diaphysis that correlate with differential mechanical requirements of a non-uniform load (strain) history. In CPL these osteon morphotypes are distinguished by variations in birefringent patterns that are attributed to their lamellar collagen organization/orientation, ranging from "hoop" osteons with a peripheral ring of highly oblique-to-transverse collagen to "distributed" osteons with highly oblique-to-transverse collagen patterns distributed across the osteon wall (Fig. 1). The scoring scheme of Martin et al. [40], which can be expressed as an

☆ This project was supported by the Doctor's Education Research Fund of Orthopaedic Hospital and the University of Southern California Department of Orthopaedic Surgery, Los Angeles, California, USA.

* Corresponding author. Utah Bone and Joint Center, 5323 South Woodrow Street, Suite 202, Salt Lake City, Utah 84107, USA. Fax: +1 801 713 0609.
E-mail address: jskedros@utahboneandjoint.com (J.G. Skedros).

8756-3282/$ – see front matter. Published by Elsevier Inc.
doi:10.1016/j.bone.2008.10.053

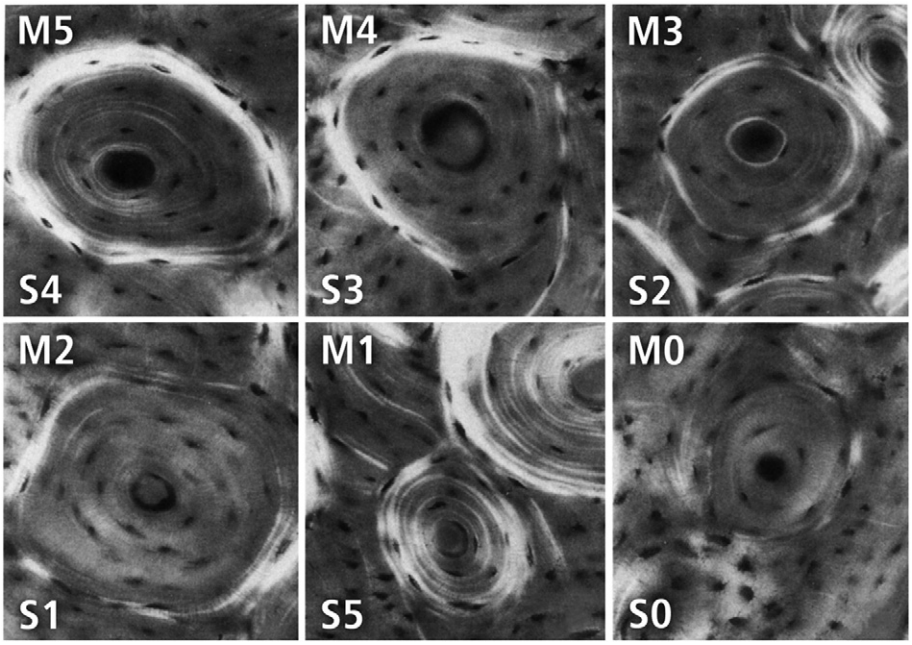

Fig. 1. Osteon morphotype/hoop scoring schemes with examples of each birefringence pattern ("morphotype"). These images are reproduced from the original study of Martin et al. [40]. The original scoring scheme from Martin et al. [40] is designated with an "M" in the upper left corner of each osteon image. The modified scoring scheme of the present study is designated with an "S" in the lower left corner of each osteon image. The section was 100 μm thick and stained *en bloc* with basic fuchsin. Each photomicrograph in this montage is to the same scale (field width 200 μm) and illustrates one of the six birefringence categories used in the present study. The numbers labeling the individual images with an "M" also represent the "hoop score" assigned to that category, in accordance with the original scheme of Martin et al. [40]: 5=category O osteon with dark interior and strongly birefringent peripheral lamellae; 4=category OI, similar to O but the birefringent ring is incomplete; 3=category OW, similar to O but the birefringent ring is weak; 2=category OWI, a combination of OI and OW; 1=category D, birefringent lamellae are distributed throughout the wall of the osteon; 0=category N, a dark osteon with no birefringent lamellae. (Reproduced from Martin et al. [40] with permission of Elsevier Science, Inc.)

'osteon morphotype score' (MTS), represents a significant advance in interpreting bone adaptation because the regional prevalence of these osteon morphotypes appears to be common, having been observed in various bones of diverse species [1,13,14,43,51,62,65,66]. It is speculated that mechanically significant regional osteon variability will be detected in many additional bones when they are eventually examined in this context.

Recent studies of cortical bone from equine MC3s have shown that spatial variations in the distributions of "hoop" and "distributed" osteons can affect regional fatigue life and toughness by differentially dissipating energy (via osteonal pullout) [25]. Results of mechanical testing coupled with histological analyses of equine radii and MC3s, and deer calcanei, also suggest that regional variations in the prevalence of these various osteon morphotypes might explain regional differences in energy absorption (a measure of "toughness") in strain-mode-specific loading (compression testing of bone habitually loaded in compression, or tension testing of bone habitually loaded in tension) [51,52,58,63]. There are two main reasons why microstructural/ultrastructural adaptations are expected for regional differences in the prevalence/predominance of strain modes (tension, compression, and shear) caused by habitual loading conditions in diaphyses of many limb bones. The first reason is that cortical (Haversian) bone exhibits marked disparities in its mechanical properties, fracture mechanics, microdamage mechanics, and microdamage accumulation with respect to tension, compression, and shear loading [17,25,50]. The second reason is that during peak loading of controlled ambulation, *in vivo* strain measurements from bones of various mammalian and avian species typically demonstrate that loading conditions can be characterized as either directionally consistent bending (tension/compression/shear) [7,30,33] where regional variations in matrix adaptation would be expected, or habitual torsion, where predominant/prevalent shear is comparatively more uniformly distributed across a bone's cross-section [33]. In the latter case, regional variation in matrix adaptation would not be expected [61].

In studies of bone adaptation using backscattered-electron and CPL images, we have typically relied on two characteristics of bone material organization to help interpret load history: population densities of secondary osteons and predominant collagen fiber orientation (CFO) (quantified as mean gray levels from the CPL birefringence of entire microscopic images from plane-parallel sections). Additionally, we have attempted to identify specific osteon morphologic variants or other histocompositional characteristics that might reflect habitual local load conditions [59,62,67]. The aim of these studies has been to determine if one or more specific characteristics of a bone's morphological organization would prove to be useful in interpreting load history, especially in limb bone cortices that are not amenable to *in vivo* strain gage analysis (e.g., fossilized bones, skeletal remains, and/or bones where technical or ethical issues preclude *in vivo* experimentation). These studies, however, have failed to detect a specific characteristic that consistently correlates with the non-uniform strain distributions of bones that are habitually loaded in bending.

In order to advance methods that rely on material characteristics for interpreting a bone's load history, we have also employed the osteon MTS scheme of Martin et al. [40]. However, in doing so we could not achieve the high correlations that would be expected between our CPL birefringence data and osteon MTSs. For example, regions with dark birefringence (dark gray levels in CPL images=low numerical values) that represent longitudinally oriented collagen in habitual "tension" regions did not correlate well with low osteon MTSs (where "dark" osteons are scored as "zero" by Martin and coworkers; Fig. 1). The main problem appeared to be the juxtaposition of a "dark" osteon's score (scored as "zero") with the score of a "bright" "distributed" osteon (scored as "one"). We concluded that the scoring scheme needed to be adjusted so that the bright "distributed" osteons (typically considered to be adaptations for habitual compression) would not confound the influence of relatively "dark" osteons (typically considered to be adaptations for habitual tension). We therefore sought to determine if a modification of this

scoring scheme, as shown in Fig. 1, would significantly enhance its utility for interpreting adaptation.

The present study evaluates how strongly these two osteon MTSs correlate with non-uniform strain environments that are experienced by many appendicular bones. We hypothesized that, in contrast to the scoring scheme of Martin et al. [40], our modified osteon MTS will strongly correlate with the prevalent/predominant strain modes (tension, compression, and shear) in bones that receive habitual bending (sheep, deer, and equine calcanei; sheep and equine radii) and weakly correlate in more complexly loaded bones where regional mechanical enhancements provided by different osteon morphotypes would not be expected because torsion/shear is comparatively prevalent (equine MC3s and sheep tibiae). Additionally, we hypothesized that our modified osteon MTS will correlate strongly with regional variations in predominant CFO, which can reliably reflect adaptation for a regionally prevalent strain mode.

Materials and methods

Bones, bone regions, strain data, and sectioning

The limb bones used are from three general/habitual load categories described by Currey [19], and represent a spectrum from relatively simple to complex loading, respectively: A) short cantilever (sheep, deer, and equine calcanei), B) curved column (equine and sheep radii), and C) straight or quasi-curved column (equine MC3s and sheep tibiae) (Fig. 2). These load categories serve to help conceptualize and simplify the characteristic loading patterns of the analyzed diaphyseal regions. Seven bones of each type were obtained from left limbs of skeletally mature animals. The equine bones were from Quarter horses

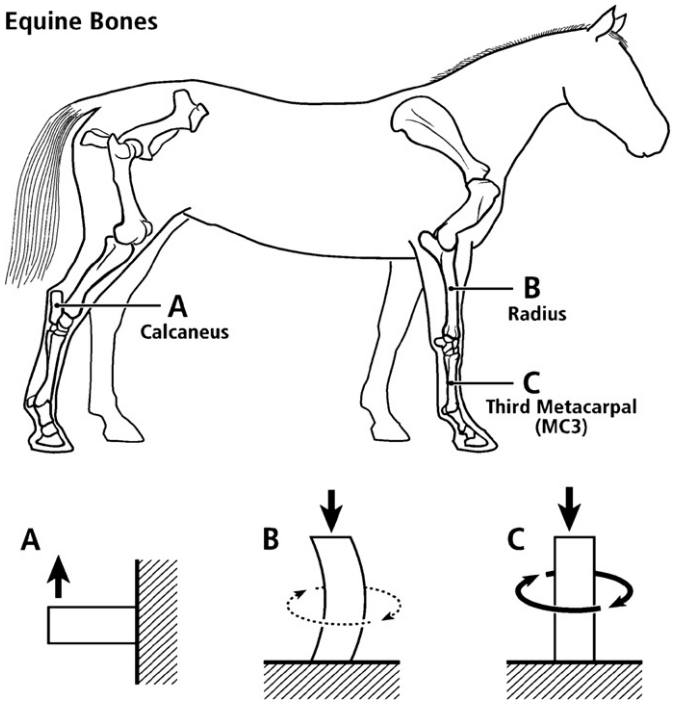

Fig. 2. Lateral-to-medial views of the right forelimb and hindlimb skeletons of an adult horse showing a spectrum from simple loading to complex loading, respectively: calcaneus (A), radius (B), and third metacarpal (MC3) (C). The drawings below are simplified renditions of each bone type, showing: (A) the calcaneus as a cantilevered beam, (B) the radius as a curved beam with longitudinal loading; the curvature accentuates bending. Torsion (dotted line) is also present but is less than the torsion in the MC3 (solid circular line in C), and (C) the MC3 with off-axis longitudinal loading producing bending and torsion, the latter being greater than in the other two bones. The mid-diaphyseal sheep tibia is also complexly loaded [31]. Several studies reporting *in vivo* strain data were used to create these drawings [8,9,24,29,53,56,72].

(4–8 years old) that were set to pasture. These animals had no history of racing or race training. Male Rocky Mountain mule deer (*Odocoileus hemionus hemionus*; estimated age range: 3–4 years) were from their natural habitat. The male sheep (*Ovis aries*) (2 years old, breed is crossed Suffolk/Hampshire and Rambouillet) were domesticated and were from large pastures. None of the animals had evidence of skeletal disease and all were killed for reasons other than limb lameness. No solutions were used to remove adherent tissues from the bones.

For purposes of the comparisons made in the present study, these bones can be separated into two groups: 1) those that experienced "habitual" bending ("tension/compression" bones), and 2) those that experienced significant torsion superimposed on bending and/or axial compression. The habitually bent bones include: A) sheep calcanei [29,68], B) equine calcanei [68], C) Rocky Mountain mule deer calcanei [70], D) sheep radii [30,32], and E) equine radii [8,51]. In these bones, axial (i.e., along the long axis of the bone) compression and axial tension are prevalent/predominant in opposing dorsal/plantar cortices (calcanei) or cranial/caudal cortices (radii).

Compared to the aforementioned "tension/compression" bones (calcanei and radii), the equine MC3s and sheep tibiae receive relatively more torsion during their habitual loading. Both of these bones also receive bending, which, in combination with torque, is most pronounced in the mid-diaphysis of the sheep tibia [31,34]. In contrast, there are studies showing that equine MC3s in some animals receive prevailing compressive strains throughout most of their mid-diaphysis during controlled locomotion [9,72]. These bones, therefore, would *not* be expected to exhibit conspicuous regional differences in predominant CFO or osteon MTS between their dorsal *vs.* palmar, and medial *vs.* lateral cortices. However, if the horses had often experienced higher activity levels (e.g. running), then significant tension can occur in the MC3 dorsal-lateral cortices [24,58]. Although none of the horses that we used had a history of racing or race training, details of their habitual activities were not known. The medial and lateral cortices of mid-diaphyseal regions of the sheep calcanei, mule deer calcanei, equine calcanei, sheep radii, and equine radii served as 'internal controls' because they would not be expected to show significant differences in microstructural or ultrastructural adaptations by being on opposing cortices of their habitual neutral axis regions where, in theory, strain magnitude and mode differences are minimal [61,68].

One five-millimeter-thick segment was cut transversely from each bone (Fig. 3). Using percentages of shaft length as described by Skedros et al. [57,68], horse and deer calcanei were each cut at the proximal third (toward the joint) of the diaphysis. Sheep and deer calcanei were cut at 70% of length, which is approximately 0.5 cm distal to the sustentaculum talus in sheep, and 1.5 cm distal in deer. Equine calcanei were cut at 60% of length, which in this bone is near the base of the sustentaculum talus. Equine and sheep radii, sheep tibiae, and equine MC3s were each cut at 50% of their overall length. These undecalcified, unstained sections were then dehydrated in ascending grades of ethanol and embedded in polymethyl methacrylate (PMMA) using standard methods [20].

Circular polarized light (CPL) analysis

Using a low speed, diamond-blade saw (Exact Instruments, West Germany) and continuous water irrigation, a one-millimeter-thick section was obtained from each PMMA-embedded segment. One surface of each of these segments was ultramilled (Reichert/Jung Ultramiller) to a high luster finish. The milled surface was mounted with cyanoacrylate glue (no other mounting substance was used) onto a glass slide and the opposite side milled to achieve a uniform overall thickness of 100±5 μm [65]. This thickness was achieved using the automated platform of the ultramiller, which provided milling at 1-micron (μm) increments that were displayed electronically on a light-emitting diode (L.E.D.) monitor. The final thickness was also verified with a digital vernier caliper (Mitutoyo™, Kanagawa, Japan).

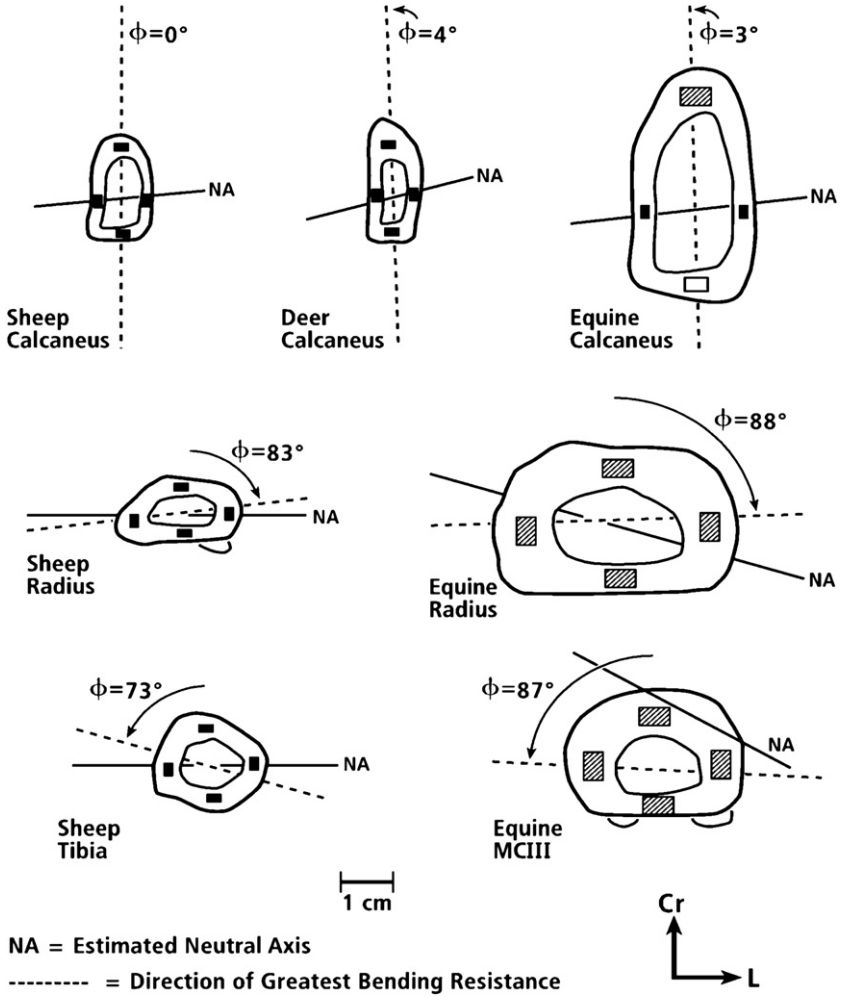

Fig. 3. Representative drawings of cross sections of: "tension/compression" bones (top five drawings), and the more complexly loaded bones (bottom two drawings). The phi (Φ) angles are the acute angles formed by the direction of greatest bending resistance (DGBR) (––) and the sagittal plane (vertical orientation in each drawing). Small rectangles (shown in three sizes) within the cortices are locations where ultrastructural/microstructural analyses were conducted. It must be noted that we use "anterior" and "posterior", respectively, as surrogates for the actual, but various, terms used for the opposing sagittal-plane cortices in the calcanei (dorsal and plantar), radii (cranial and caudal), and equine MC3 (dorsal and palmar). Cr=cranial, anterior, or dorsal, L=lateral.

Milled sections were analyzed for CFO using CPL according to the method of Boyde and Riggs [13], where they were viewed in the light microscope after being placed between appropriately crossed left and right hand polarizing filters (HNCP37×0.030inch (0.762 mm) filter; Polaroid Corporation, Norwood, MA) [45]. Regional differences in CFO were quantified in terms of corresponding differences in the transmitted light intensity, where darker gray levels represented relatively more longitudinal CFO and brighter gray levels represent relatively more oblique-to-transverse CFO [13,14]. This method assumes that all other factors that can artifactually change the intensity of transmitted light (e.g., variations in specimen thickness) are eliminated.

Gray level values and other microstructural parameters were quantified in the mid-cortex of the anterior, posterior, medial, and lateral locations of each section (Fig. 3). It must be noted that we use "anterior" and "posterior", respectively, as surrogates for the actual, but various, terms used for the opposing sagittal-plane cortices in the calcanei (dorsal and plantar), radii (cranial and caudal), and equine MC3 (dorsal and palmar). Four 50x images (512 by 480 pixels; approximately 2.3 mm by 2.3 mm images) were analyzed for most cortical locations. A 4× objective was used with a 0.10 numerical aperture (Olympus "D-Plan 4X, 0.10, 160/.17"), which provided 15.5 μm depth of field. For each image, the region analyzed was adjusted so that only the bone from the central 80% of the cortex was quantified. For example, care was taken to avoid the variably present, highly birefringent circumferential lamellar bone.

Because some bones had relatively thin cortices, fewer than four images could be analyzed: three in the equine calcaneal plantar cortex and two in each of the equine calcaneal medial and lateral cortices, two in each of the sheep radii and tibiae cortical regions, and two in each of the deer and sheep calcanei cortical regions. In order to ensure minimal sampling error within cortical locations [27], pilot studies were conducted to confirm that the number of images selected in any given cortical region accurately accounted for over 95% of the local microstructural variation.

Using hardware-based algorithms of a computerized imaging system (Image 1, Universal Imaging Corporation, West Chester, PA) and a video camera and monitor (Sony Video Camera, Model DXC-750MD; Sony Trinitron Color Video Monitor, Model PVM-1343MD, Japan), the grayscale images from each cortex were digitized directly from the microscope and stored onto a re-writable optical disc (Panasonic Optical Disk Cartridge, LM-D702W, Japan). Uniformity and consistency of the light source across the entire field of view was periodically verified using the hardware-based algorithms of this imaging system [65].

According to published methods [13,65], predominant CFO was determined from CPL images using sections obtained from each bone. One 50X image was obtained in each octant. Regional differences in CFO

were inferred from corresponding differences in the intensity of transmitted light (based on the relative intensity of birefringence), where darker gray levels (lower numerical values) represent relatively more longitudinal collagen, and brighter gray levels (higher numerical values) represent relatively more oblique-to-transverse collagen. Gray level values are represented as integers from 0, 1, 2, 3, … 255. The methods used to determine a weighted mean gray level (WMGL) from each image have been described elsewhere [10,65]. These methods include the elimination of gray level values (gray level values 20 or less) that represent tissue voids such as vascular canals and lacunae. The PMMA-filled porous spaces, which were dark/non-birefringent in CPL, were also eliminated by this gray-level thresholding method. Boyde and Riggs [13] have shown that these methods produce similar relative differences between anterior ("tension" = dark gray-levels) and posterior ("compression" = bright gray-levels) cortices of mineralized and demineralized PMMA-embedded sections of equine radii. The methods used to quantify regional CFO differences in cortical bone as differences in gray levels [14,65] have produced relative absolute differences that are similar to the "longitudinal structure index" used to describe differences in predominant CFO by Martin et al. [42], Takano et al. [71], and Kalmey and Lovejoy [28]. In the present study, regional variations in image gray levels are referred to as differences in "CFO/WMGL".

Microstructure analysis: osteon selection criteria and osteon morphotype score

Microscopic images stored on the optical disc were printed on paper (HP LaserJet Series II printer, Hewlett-Packard Co., Boise, ID). By viewing the actual microscopic fields and using their printed images as guides, the perimeters of complete secondary osteons (Haversian systems) were traced on transparent sheets. The investigator (JGS) who performed all of the tracings had been studying osteon morphology for over 15 years. In pilot analyses it had been established that his intra-observer error was < 1.5%. A Hewlett-Packard scanner (ScanJet Plus, Model HP9195A, Firmware 2917, Japan) and Scangal Gallery Plus 5.0 software (Version A.05.05, Hewlett-Packard, Palo Alto, CA) was used to digitize the tracings.

Since the mechanical properties of primary (un-remodeled) or poorly remodeled bone differ from those of more highly remodeled (secondary osteon) bone [18], it is important to distinguish the primary osteons of primary bone from secondary osteons of remodeled bone. Because secondary osteons are formed through a resorption and replacement process, their outer margin will often intersect lamellae of the surrounding bone. Since this type of intersection is not seen in primary bone, secondary bone (secondary osteons and secondary osteon fragments) can be readily distinguished from primary bone in most instances. Additionally, secondary osteons can usually be distinguished from primary osteons by various other mutually exclusive characteristics including their reoriented collagen matrix (as seen in polarized light) and their highly mineralized circumferential margin traditionally known as the cement line. By definition, primary osteons do not have cement lines [60].

The criteria for selecting a secondary osteon were in accordance with those described by Martin et al. [40], and included: 1) presence of a scalloped cement line, 2) absence of a Volkmann's canal connection, 3) reasonably circular or ellipsoid shape, and 4) refilling complete or nearly so. Each secondary osteon that was both complete and met these criteria (>10,000 total osteons) was placed into one of six categories, based on birefringence pattern (Fig. 1). Three trained

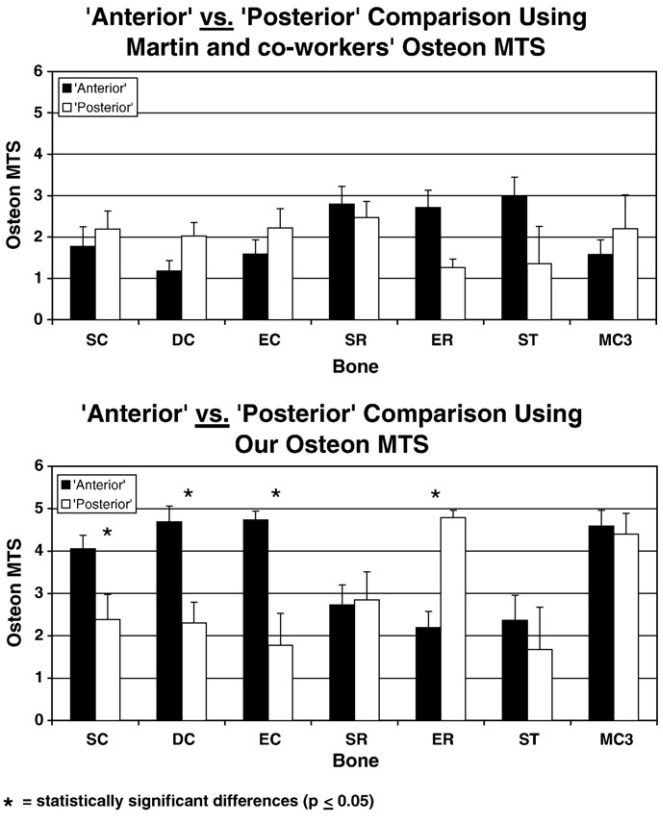

Fig. 4. Means and standard deviations (narrow vertical line) of anterior *vs.* posterior differences in osteon MTSs using Martin and co-workers' [40] and our osteon MTS schemes in various species and bones. SC = sheep calcaneus, DC = deer calcaneus, EC = equine calcaneus, SR = sheep radius, ER = equine radius, ST = sheep tibia, MC3 = equine third metacarpal. No statistically significant anterior-posterior differences were found when using Martin et al. original score (Top Figure).

investigators made these determinations. Training included blinded assessments using images from all bones with close supervision by the principal investigators (SDM, JGS), and were repeated until intra-observer and inter-observer discrepancies were less than 2.5%. All osteons with uncertain morphology were designated to one of the categories after a consensus opinion was reached (SDM, JGS).

Each osteon type was then assigned a numerical value in accordance with two scoring schemes. The first was Martin and co-workers' numerical values: dark = 0, distributed = 1, weak incomplete hoop = 2, weak hoop = 3, incomplete hoop = 4, and hoop = 5 ("weak" or "incomplete" refer to a weak or incompletely present hoop at the osteon periphery) (see values indicated with "M" in Fig. 1). The second was our modified osteon scoring scheme: dark = 0, weak incomplete hoop = 1, weak hoop = 2, incomplete hoop = 3, hoop = 4, and distributed = 5 (see values indicated with "S" in Fig. 1). This modification juxtaposes morphotypes associated with overall increased birefringence (increased oblique-to-transverse CFO). We considered these adjustments to be most relevant for the purposes of the present study; namely, using histomorphometric parameters to infer strain-mode-related (compression *vs.* tension) adaptation in habitually bent bones [43,62,66]. The numerical designations for the osteon morphotypes were tabulated using each scheme, and then the two different osteon MTSs were calculated for each image. This was

Fig. 5. Means and standard deviations of regional differences in osteon morphotype score (MTS), osteon population density (On.N/T.Ar, in brackets above the bars), and CFO/WMGL in: (A) sheep calcanei, (B) deer calcanei, (C) equine calcanei, (D) sheep radii, (E) equine radii, (F) sheep tibiae, and (G) our equine MC3s. Statistically significant differences between paired comparisons are indicated by the abbreviations shown within a bar (osteon MTS and CFO/WMGL), or as superscripts in the brackets above the bars (On.N/T.Ar). For example, for the CFO/WMGL data in the dorsal cortex of the sheep calcaneus (dark bar at far left of A) the letters P, M, and L show that the dorsal (D) cortex is significantly different from the plantar, medial, and lateral cortices, respectively.

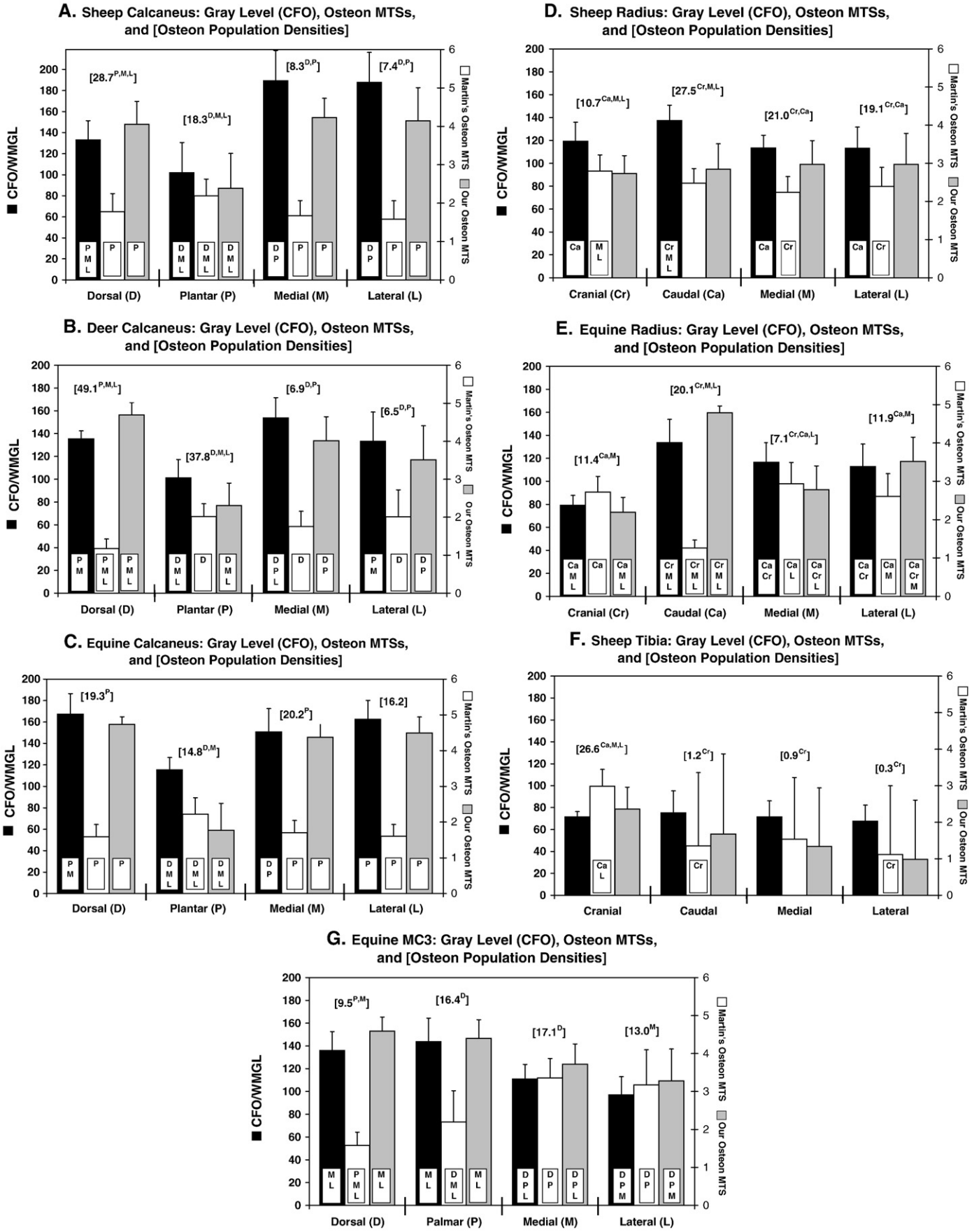

accomplished by determining the number of each specific osteon type, multiplying each type by its respective assigned value (0, 1, 2, [5], summing the products, and then dividing by the total number of quantified osteons [40].

Statistical analysis

Birefringence pattern (osteon morphotype) data were analyzed in several ways. A two-factor analysis of variance (ANOVA) was conducted for each parameter in each species using region (anterior, posterior, medial, lateral) and animal. All possible pair-wise comparisons between cortical regions and each of the other parameters (CFO/WMGL, On.N/T.Ar, Martin's MTSs, our MTSs) in each species were then assessed for statistical significance using Fisher's Least Significant *post-hoc* test [69] (Stat View Version 5.0, SAS Institute Inc., Cary, NC). An alpha level of <0.05 was considered statistically significant. Pearson correlation coefficients (r values) were determined for various comparisons between CFO/WMGL and osteon MTS. The magnitudes of the resulting correlation coefficients (r) were interpreted according to the classification of Hinkle et al. [26]. In this scheme, coefficients in the ranges of 0.9 to 0.99, 0.7 to 0.89, 0.5 to 0.69, 0.3 to 0.49, and 0.0 to 0.29 are interpreted as representing very high, high, moderate, low, and little if any correlation, respectively.

Results

Paired comparisons with osteon morphotype scores (MTSs) and two-way ANOVA results

Results of regional comparisons are summarized in Figs. 4 and 5, and representative CPL images showing osteon morphotypes are shown in Fig. 6. In Table 1A are the raw numbers for the various osteon categories reported in equine MC3s by Martin et al. [40] and in Tables 1B–C are the numerical tabulations of the two scoring schemes. Results of two-way ANOVA analyses (animal, region) showed that 'animal' had a significant effect in the context of each parameter (Martin's osteon MTSs, our MTSs, On.N/T.Ar, and CFO/WMGL) in each species except for the equine calcanei and sheep tibiae. Examination of scatter plot data from each parameter in each of the remaining species revealed that this effect of 'animal' was typically the result two or fewer bones with a relatively increased difference between anterior/posterior data when compared to medial/lateral data. A significant effect of 'region' (anterior, posterior, medial, lateral) was also shown in all species except for the sheep tibiae. The subsequent analyses focus on the effect of 'region' for each parameter after blocking the affect of 'animal'.

In contrast to the original scoring scheme of Martin et al. [40], our modified scoring scheme revealed significant anterior/posterior differences in osteon MTSs in nearly all habitually bent ("tension/compression") bones ($p<0.0001$) (Fig. 4). The sheep radii were the only exception, where the anterior/posterior comparison was not statistically significant ($p=0.11$). Examination of the CPL images of these radii suggested that, in contrast to the other "tension/compression" bones, the bright birefringence produced by the relatively greater amount of un-remodeled bone (i.e. lower osteon population density), especially in the anterior (cranial) cortex, contributed to this unexpected result.

In the more complexly loaded bones (equine MC3s and sheep tibiae, Figs. 2 and 4), anterior/posterior differences were also, as expected, not statistically significant. However, in comparison to sheep tibiae where no significant differences were found (or expected) in the modified osteon MTS in *all* possible region comparisons, our equine MC3s showed *un*expected significant differences between medial *vs.* lateral cortices with higher osteon MTSs in the medial cortex ($p<0.001$). This result, as discussed below, may reflect a habitual strain distribution in our MC3s that is produced by a neutral axis that rotates: 1) less than expected during locomotion, and 2) is oriented relatively more anterior-to-posterior than what was predicted — resulting in prevalent/predominant compression in the medial cortex and tension in the lateral cortex.

Using the equine MC3 data from Martin et al. [40], we compared regional differences using our scoring system and their original scoring scheme (Table 1). When using our scoring scheme, a more substantial and inverse difference was revealed between the dorsal and lateral regions (higher osteon MTS in dorsal than lateral) (Fig. 7). This result, in contrast with Martin and co-worker's dorsal/lateral difference (lower osteon MTS in dorsal than lateral), can be attributed to the fact that our score revealed significantly higher osteon MTSs in the dorsal region, and significantly lower osteon MTSs in the lateral region. This result might reveal a dorsal/lateral compression/tension adaptation that was not revealed by the original score. In turn, the original score showed a significant dorsal/medial difference (Fig. 7), which was not revealed by the modified score. As discussed below, the minor dorsal/medial difference revealed by the modified score might more accurately reflect the prevalent/predominant compression in both of these locations.

Correlations with osteon MTSs

In support of our second hypothesis, the modified osteon MTS correlates more strongly with the local predominant CFO/WMGL of a strain distribution of habitual bending than does the original scoring scheme. Correlations between the osteon MTSs that were calculated using the scoring scheme of Martin et al. [40] (using our images) with our CFO/WMGL data from *all* regions of *each* bone type also invariably demonstrated weak-to-moderate *negative* correlations (Table 2). In contrast, typically high *positive* correlations were found when the same comparisons were made between the modified osteon MTSs and the regional CFO/WMGL data.

Osteon population densities: paired comparisons and correlations

Results of regional comparisons of secondary osteon population densities (On.N/T.Ar) and CFO/WMGL are summarized in Figs. 5A–G. These results show that in all "tension/compression" bones (i.e. calcanei and radii), On.N/T.Ar is significantly greater in the "compression" cortex than in the "tension" cortex ($p<0.05$). However, in these "tension/compression" bones, CFO/WMGL and On.N/T.Ar are negatively and weakly correlated ($r=-0.194$; $p<0.05$). When the equine bones are eliminated from this analysis, and only the calcanei are retained, the correlation between CFO/WMGL and On.N/T.Ar becomes even more negative ($r=-0.432$; $p<0.001$). In other words, as On.N/T.Ar decreases, CFO/WMGL increases (becomes brighter=more oblique-to-transverse CFO). These negative correlations starkly contrast with the positive correlations between the CFO/WMGL and osteon MTS data.

Discussion

In support of our first hypothesis, when compared to the original scoring scheme of Martin et al. [40], the modified osteon morphotype score (MTS) more clearly demonstrated differences between the "tension" *vs.* "compression" cortices of the habitually bent bones. This hypothesis is also supported by the accentuated and reversed dorsal *vs.* lateral differences that the modified osteon MTS revealed in a re-analysis of the equine MC3 osteon data reported by Martin and co-workers. The reasons for these differences are readily understood in the context of the modified scoring scheme where the numerical juxtaposition of the strongly hooped secondary osteons (i.e., those with the bright, highly oblique-to-transverse, peripheral osteonal lamellae) *and* the bright "distributed" osteons (i.e., with highly oblique-to-transverse CFO throughout the osteon wall) account for the high osteon MTSs in the habitually compressed cortices of nearly

all bones, and the numerical juxtaposition of weakly hooped secondary osteons *and* the more prevalent "dark" osteons account for the low osteon MTSs in the habitually tension-loaded cortices of nearly all bones. Although sheep radii are an exception in the context of these anterior/posterior strain-mode-related comparisons, the strength of the correlation of osteon MTSs with CFO/WMGL in these bones was still significant ($p<0.05$) even though it was comparatively weak ($r=0.343$). This result can be attributed to the oblique-to-transverse CFO in the anterior (cranial) "tension" cortex that is influenced by highly birefringent/oblique-to-transverse collagen in the primary (un-remodeled) bone (Fig. 6).

As expected, the correlation in our equine MC3s between osteon MTS and CFO/WMGL was also comparatively weak. However, the medial *vs.* lateral difference in osteon MTSs in our equine MC3s was

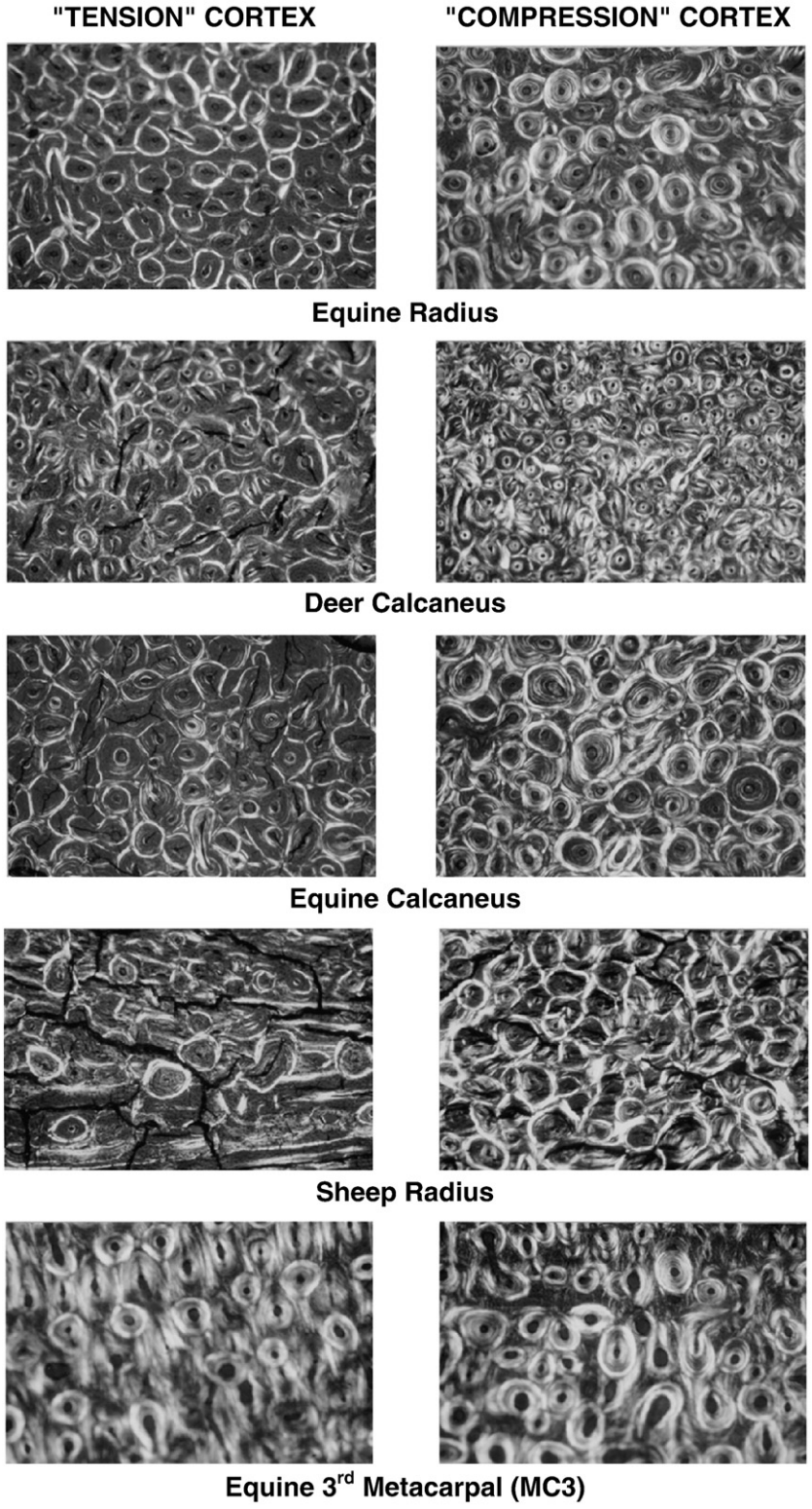

Fig. 6. Representative circularly polarized light (CPL) images of bone from "tension" cortices (at left) and "compression" cortices (at right). All images are taken under identical illumination and 50x magnification. Bone in the sections is un-decalcified and the sections are unstained; the width of each image is ~1.52 mm.

Table 1

A. Martin et al. [40] raw numbers: contingency table for regional distribution of osteon categories

Region	Osteonal categories						
	O	OI	OW	OWI	D	N	Sum total
Dorsal	23	6	16	15	48	12	120
Medial	44	18	32	11	14	1	120
Lateral	26	14	39	34	2	5	120
Total	93	38	87	60	64	18	360

B. Cumulative values using Martin et al. "hoop score"[†]

Region	Osteonal categories with original numerical assignment							
	O*5	OI*4	OW*3	OWI*2	D*1	N*0	Sum total	Hoop score[†]
Dorsal	115	24	48	30	48	0	265	2.21
Medial	220	72	96	22	14	0	424	3.53
Lateral	130	56	117	68	2	0	373	3.11
Total	465	152	261	120	64	0	1062	2.95

C. Cumulative values using our osteon morphotype Score (MTS)[‡]

Region	Osteonal categories with our numerical assignment							
	O*4	OI*3	OW*2	OWI*1	D*5	N*0	Sum total	Hoop score[†]
Dorsal	92	18	32	15	240	0	397	3.31
Medial	176	54	64	11	70	0	375	3.13
Lateral	104	42	78	34	10	0	268	2.23
Total	372	114	174	60	320	0	1040	2.89

O=strong complete hoop.
OI=strong incomplete hoop.
OW=weak hoop.
OWI=weak incomplete hoop.
D=distributed.
N=dark (no hoop or birefringent lamellae).
(See legend of Fig. 1 for further description of these categories).
Note that the "Hoop Score" (=osteon MTS) values in B are slightly different from the Hoop Score values in Martin and co workers' actual table (their Table 2). The reason for this is that the values of Martin et al. are based on averages from ten osteons within each section (probably mean of 12 sections), while our calculations of his average Hoop Score were derived from the aggregate values provided in their contingency table (A above).
[†] The raw values used in these calculations are from A above.
[‡] As described in the text, our osteon MTS is determined using a scoring scheme that is different from that of Martin et al. [40]. Our scoring scheme: N=0, OWI=1, OW=2, OI=3, O=4, D=5.

larger than expected ($p=0.02$). This result might be attributed to *in vivo* strain data suggesting that in some horses the neutral axis typically courses in a more anterior-posterior direction than in a medial-lateral direction [58]. This anterior-posterior orientation would load the medial and lateral cortices in prevalent/predominant compression and tension, respectively (the neutral axis would tend toward vertical in the equine MC3 cross-section depicted in Fig. 3).

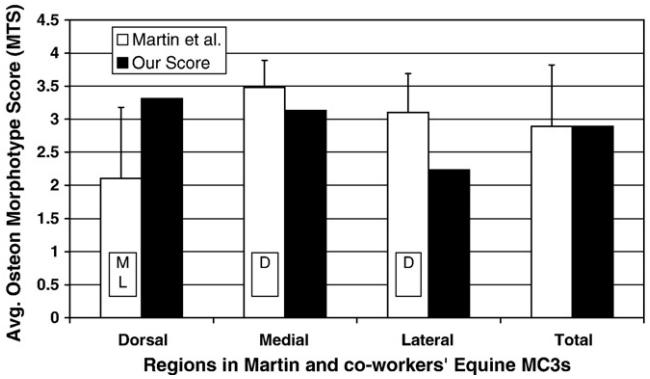

Fig. 7. Regional variations in osteon MTSs between Martin and et al. [40] and our scoring schemes using their equine MC3 data. Note that Martin et al. only examined the dorsal (anterior), medial, and lateral cortices; in the present study we also analyzed the palmar (posterior) cortices of our MC3s. The results of their statistical analyses are shown, where: 1) dorsal *vs.* lateral, $p=0.009$; 2) dorsal *vs.* medial, $p=0.001$; 3) medial *vs.* lateral is not significant. Note that our data show only mean values because in Martin et al. [40] the reported data are insufficient for determining statistical differences and standard deviations.

This possibility has been offered as an explanation for why Martin and co-workers' equine MC3s (from racing or retired-racing Thoroughbreds) [[23] and Table 1 therein] do not exhibit the relatively more consistent dark birefringence ("tension" CFO) in the lateral cortex that has been reported in our previous work [58,65] in mixed breeds of non-racing non-thoroughbred horses.

The absence of strong correlations in all regions analyzed in the sheep tibiae was expected — it is presumed that the more prevalent shear stress (as a result of a broadly shifting neutral axis caused by relatively increased load complexity) would be accommodated by relative spatial uniformity of CFO and/or osteon morphotypes [61]. In other words, in these bones the 'adaptive state' would be relative uniformity in collagen organization/orientation, which is consistent with the idea that *regional* strain-mode-related tissue-level enhancements for fatigue resistance and toughness, whether provided by osteons or by the primary bone, would not be required in habitual shear environments.

Table 2
CFO/WMGL vs. Osteon MTS Correlation Coefficients (r values)

Bone	Martin et al.	Our score
Sheep calcaneus	−0.543*	0.806*
Deer calcaneus	−0.396*	0.757*
Equine calcaneus	−0.525*	0.809*
Equine radius	−0.318*	0.764*
Sheep radius	0.055	0.343*
Equine MC3	−0.517*	0.672*
Sheep tibia	−0.216	−0.061

* $p<0.05$.

Mechanical relevance of regional variations in osteon morphotypes

The genesis of studies showing differential mechanical properties of osteon morphotypes can be traced to those of Ascenzi and Bonucci [2,3]. These investigators elucidated a correlation between the mechanical properties of *individual* secondary osteons and the birefringence patterns that they identified: predominantly bright, predominantly dark, or alternating bright and dark lamellae. They observed, for example, that the *dark* osteons had greater strength in *tension* than those having bright or "alternating lamellae". Following the interpretation of lamellar structure postulated by von Ebner [76] and Gebhardt [22], osteons with alternating lamellae, as seen when viewed between crossed polarizers, were assumed to have plies in which the collagen fibers alternated between longitudinal and transverse directions. Osteons appearing entirely bright or dark were assumed to have mostly transverse or longitudinally oriented fibers, respectively [14], although alternative explanations have been postulated [4,5,36,73].

Several subsequent investigators studied the relationship between CFO and mechanical properties of macroscopic cortical bone specimens. For example, studies of cortical bone anisotropy using plane-polarized light have shown that predominant CFO is correlated with mechanical properties of tested specimens, including strength or failure strain [1,21,48,49]. Martin and Ishida [41] also quantified birefringence with plane-polarized light and reported that longitudinal CFO was an important predictor of tensile strength in bovine cortical bone. Martin and Boardman [37] found similar results for the bending strength and elastic modulus of bovine cortical bone. Using four-point-bending to test beams cut from equine radial diaphyses, and both CPL and plane-polarized light analyses of tested specimens, Martin et al. [42] showed that longitudinally oriented collagen correlated with greater modulus and monotonic strength.

In sum, these studies reflect conventional wisdom that the *in vivo* role for predominant CFO is primarily for affecting strength- or stiffness-related material properties. In contrast, recent studies using strain-mode-specific loading (i.e., compression testing of bone habitually loaded in compression, and tension testing of bone habitually loaded in tension) suggest that CFO may more strongly influence regional material toughness (energy absorption). In a study of mid-diaphyseal cortical specimens of mature equine MC3s in our laboratory [58], we examined the relative contributions of multiple material characteristics (CFO/WMGL, porosity, % ash, On.N/T.Ar, On.Ar/T.Ar, and individual osteon cross-sectional area) in strain-mode-specific testing. In tension testing (dumbbell specimens), CFO/WMGL was one of the top three characteristics in explaining variability in yield stress, ultimate stress, ultimate energy absorption, and total energy absorption. In compression testing (cube specimens), CFO/WMGL was among the top three characteristics in explaining yield energy absorption, ultimate energy absorption, and total energy absorption. These results add to a growing body of experimental data that reveal an important role for predominant CFO, collagen content, and/or intermolecular collagen cross-links in affecting energy absorption (a measure of "toughness") [6,15,47,77].

In comparison to these studies of the mechanical importance of regional variations in averaged CFO/WMGL values, there is only one study that we are aware of that specifically evaluates the impact of specific osteon morphotypes (as observed in CPL images) on tissue mechanical properties. In this study, Hiller, Martin et al. [25] showed that variations in the distributions of "hooped" and "distributed" osteons in dorsal, medial, and lateral cortices of equine MC3s can affect regional fatigue life and toughness by differentially dissipating energy (via osteonal pullout). This correlates well with the suggestion that variations in the prevalence of specific osteon morphotypes might explain regional differences in CFO/WMGL that clearly influence energy absorption in strain-mode-specific testing [58].

The confounding influence of strain magnitude: Can osteon morphotypes adapt bone for regional variations in strain magnitude?

Large differences in strain *magnitude* between opposing cortices (compression>tension) and across each of the bones that we examined may be important factors for the development of the regional differences in their predominant CFO, osteon morphotypes, and/or On.N/T.Ar. It is clear that the functional use of limb long bones often results in axially directed loads with superimposed bending, producing larger strain magnitudes in the "compression" cortex than in the "tension" cortex [34]. Consequently, the co-existence of variations in strain mode and strain magnitude are often inextricably linked, thus complicating simple/straight-forward interpretations of the development of strain-specific adaptations in many limb bones to such an extent that causal relationships are difficult to determine. For example, Martin and Burr [38], Mason et al. [43], and Main [35] note that such a combination precludes simple interpretations for the high On.N/T.Ar that occur in more highly strained "compression" cortices of many bones loaded in habitual bending. If strain magnitude is important in this context, then it is difficult to explain, for example, why relatively high concentrations of osteons occur in the anterior (cranial) cortex of the sheep tibiae (Fig. 5F) because walking produces peak tension and compression strain magnitudes that are nearly equivalent in the cranial and caudal cortices. However, during faster gaits the sheep tibia experiences peak principal *tensile* strains on the cranial cortex that are approximately 30% *larger* than peak compressive strains on the caudal cortex [31,34]. Regional differences in some osteon-related characteristics may be the result of physiologic processes evolutionarily selected for eliminating or minimizing some potentially harmful mechanical (e.g., high strains) and/or tissue effects (e.g., microdamage) [11,16,46,54,55]. If this interpretation is correct, then the stimuli responsible for observed adaptive differences across a bone section may no longer be present in mature bones. Controlled studies of skeletal development are needed to clarify these issues in the contexts of regional variations in predominant CFO, On.N/T.Ar, and osteon morphotypes.

Results of the present study are sufficiently compelling for us to suggest that osteon remodelling produces regional variations in osteon morphotypes and associated regional variations in CFO/WMGL. Ontogenetic evidence supporting this idea has been described in equine and sheep radii [51,64], and sheep and deer calcanei [62,66]. But there are also examples where apparent tension *vs.* compression differences in CFO/WMGL have been quantified in locations of some bones where osteons are absent or few; e.g., in metaphyseal-diaphyseal locations of equine radii [43] and in mid-diaphyses of turkey ulnae [61]. Hence, it cannot be concluded that only the osteon remodeling process produces variations in CFO/WMGL because modeling (the formation of primary bone) in some bones appears to achieve this regional ultrastructural variability. But in these exceptional cases, it is not known if this regional variability in the primary bone birefringence has mechanical consequences that are comparable to the regional "toughening" that is produced by differences in secondary osteon morphotypes. Regional toughening and fatigue life can also be affected by variations in osteon diameter [23,25]. This affect appears to be related to the shear strength in the cement line region and the phenomenon of osteon pullout. Enhancements of shear strength of the osteon periphery in this context (especially with respect to hooped osteons), and the differential and interactive effects of osteon size and morphotype have been reported in mechanical testing studies of equine MC3s [25]. These relationships, which were not explored in the present study, warrant further investigation. Although, there are finite element studies suggesting that strain magnitude variations influence remodeling dynamics that ultimately affect osteon size [74,75], we could not locate similar studies that suggest or imply that specific strain characteristics (e.g. mode) might be closely involved in affecting the differential production of the morphotypes that we describe in our

bones. Additional studies are needed to determine the mechanisms that causally mediate osteoblasts to produce these regional matrix heterogeneities in these various bones, and to further elucidate their ultimate mechanical consequences.

Acknowledgments

The authors thank Wm. Erick Anderson, Kyle Gubler, Jaxon Hoopes, and Scott Sorenson for their assistance in completing this study. We are also grateful for the insightful discussions of David Burr, Harry McKellop, and Edward Ebramzadeh. We are indebted to Pat Campbell and Harlan Amstutz for the use of their laboratory facilities at the Joint Replacement Institute of Orthopaedic Hospital in Los Angeles, California.

References

[1] Ascenzi A. The micromechanics versus the macromechanics of cortical bone–a comprehensive presentation. J Biomech Eng 1988;110:357–63.
[2] Ascenzi A, Bonucci E. The compressive properties of single osteons. Anat Rec 1968; 161:377–91.
[3] Ascenzi A, Bonucci E. The tensile properties of single osteons. Anat Rec 1967;158: 375–86.
[4] Ascenzi MG, Ascenzi A, Benvenuti A, Burghammer M, Panzavolta S, Bigi A. Structural differences between “dark” and “bright" isolated human osteonic lamellae. J Struct Biol 2003;141:22–33.
[5] Ascenzi MG, Lomovtsev A. Collagen orientation patterns in human secondary osteons, quantified in the radial direction by confocal microscopy. J Struct Biol 2006;153:14–30.
[6] Banse X, Sims TJ, Bailey AJ. Mechanical properties of adult vertebral cancellous bone: correlation with collagen intermolecular cross-links. J Bone Miner Res 2002;17:1621–8.
[7] Biewener AA, Bertram JEA. Mechanical loading and bone growth *in vivo*. In: Hall BK, editor. Bone Growth - B. Bone, vol. 7. Boca Raton, FL: CRC Press; 1993. p. 1–36.
[8] Biewener AA, Thomason J, Goodship A, Lanyon LE. Bone stress in the horse forelimb during locomotion at different gaits: a comparison of two experimental methods. J Biomech 1983;16:565–76.
[9] Biewener AA, Thomason J, Lanyon LE. Mechanics of locomotion and jumping in the forelimb of the horse (*Equus*): *In vivo* stress developed in the radius and metacarpus. J Zool Lond 1983:67–82.
[10] Bloebaum RD, Skedros JG, Vajda EG, Bachus KN, Constantz BR. Determining mineral content variations in bone using backscattered electron imaging. Bone 1997;20:485–90.
[11] Bouvier M, Hylander WL. The mechanical or metabolic function of secondary osteonal bone in the monkey *Macaca fascicularis*. Arch Oral Biol 1996;41:941–50.
[12] Boyde A, Bianco P, Portigliatti Barbos M, Ascenzi A. Collagen orientation in compact bone: I. A new method for the determination of the proportion of collagen parallel to the plane of compact bone sections. Metab Bone Dis Relat Res 1984;5:299–307.
[13] Boyde A, Riggs CM. The quantitative study of the orientation of collagen in compact bone slices. Bone 1990;11:35–9.
[14] Bromage TG, Goldman HM, McFarlin SC, Warshaw J, Boyde A, Riggs CM. Circularly polarized light standards for investigations of collagen fiber orientation in bone. Anat Rec 2003;274B:157–68.
[15] Burr DB. The contribution of the organic matrix to bone's material properties. Bone 2002;31:8–11.
[16] Burr DB. Remodeling and the repair of fatigue damage. Calcif Tissue Int 1993;53: S75–81.
[17] Burstein AH, Currey JD, Frankel PVH, Reilly DT. The ultimate properties of bone tissue: effects of yielding. J Biomech 1972;5:35–44.
[18] Currey JD. Bones: Structure and mechanics. Princeton, NJ: Princeton University Press; 2002.
[19] Currey JD. Can strains give adequate information for adaptive bone remodeling? Calcif Tissue Int 1984;36:S118–22.
[20] Emmanual J, Hornbeck C, Bloebaum RD. A polymethyl methacrylate method for large specimens of mineralized bone with implants. Stain Tech 1987;62:401–10.
[21] Evans FG, Vincentelli R. Relations of the compressive properties of human cortical bone to histological structure and calcification. J Biomech 1974;7:1–10.
[22] Gebhardt W. Über funktionell wichtige anordnungsweisen der feineren und görberen bauelemente des wirbeltierknochens. II. Spezieller teil. Der bau der Haversschen lamellensysteme und seine funktionelle bedeutung. Arch Entwicklungsmech Org 1906;20:187–322.
[23] Gibson VA, Stover SM, Gibeling JC, Hazelwood SJ, Martin RB. Osteonal effects on elastic modulus and fatigue life in equine bone. J Biomech 2006;39:217–25.
[24] Gross TS, McLeod KJ, Rubin CT. Characterizing bone strain distribution *in vivo* using three triple rosette strain gauges. J Biomech 1992;25:1081–7.
[25] Hiller LP, Stover SM, Gibson VA, Gibeling JC, Prater CS, Hazelwood SJ, et al. Osteon pullout in the equine third metacarpal bone: Effects of *ex vivo* fatigue. J Orthop Res 2003;21:481–8.
[26] Hinkle DE, Wiersma W, Jurs WG. Applied statistics for the behavioral sciences. Chicago, IL: Rand McNally College Pub. Co.; 1979.
[27] Iwaniec UT, Crenshaw TD, Schoeninger MJ, Stout SD, Ericksen MF. Methods for improving the efficiency of estimating total osteon density in the human anterior mid-diaphyseal femur. Am J Phys Anthropol 1998;107:13–24.
[28] Kalmey JK, Lovejoy CO. Collagen fiber orientation in the femoral necks of apes and humans: do their histological structures reflect differences in locomotor loading? Bone 2002;31:327–32.
[29] Lanyon LE. Experimental support for the trajectorial theory of bone structure. J Bone Joint Surg 1974;56B:160–6.
[30] Lanyon LE, Baggott DG. Mechanical function as an influence on the structure and form of bone. J Bone Joint Surg 1976;58-B:436–43.
[31] Lanyon LE, Bourn S. The influence of mechanical function on the development and remodeling of the tibia: an experimental study in sheep. J Bone Joint Surg 1979;61-A:263–73.
[32] Lanyon LE, Magee PT, Baggott DG. The relationship of functional stress and strain to the processes of bone remodeling: an experimental study on the sheep radius. J Biomech 1979;12:593–600.
[33] Lieberman DE, Pearson OM, Polk JD, Demes B, Crompton AW. Optimization of bone growth and remodeling in response to loading in tapered mammalian limbs. J Exp Biol 2003;206:3125–38.
[34] Lieberman DE, Polk JD, Demes B. Predicting long bone loading from cross-sectional geometry. Am J Phys Anthropol 2004;123:156–71.
[35] Main RP. Ontogenetic relationships between *in vivo* strain environment, bone histomorphometry and growth in the goat radius. J Anat 2007;210:272–93.
[36] Marotti G. The structure of bone tissues and the cellular control of their deposition. Ital J Anat Embryol 1996;101:25–79.
[37] Martin RB, Boardman DL. The effects of collagen fiber orientation, porosity, density, and mineralization on bovine cortical bone bending properties. J Biomech 1993;26:1047–54.
[38] Martin RB, Burr DB. Structure, Function and Adaptation of Compact Bone. New York: Raven Press; 1989.
[39] Martin RB, Burr DB, Sharkey NA. Skeletal Tissue Mechanics. New York, NY: Springer-Verlag; 1998.
[40] Martin RB, Gibson VA, Stover SM, Gibeling JC, Griffin LV. Osteon structure in the equine third metacarpus. Bone 1996;19:165–71.
[41] Martin RB, Ishida J. The relative effects of collagen fiber orientation, porosity, density, and mineralization on bone strength. J Biomech 1989;22:419–26.
[42] Martin RB, Mathews PV, Lau ST, Gibson VA, Stover SM. Collagen fiber organization is related to mechanical properties and remodeling in equine bone. A comparison of two methods. J Biomech 1996;29:1515–21.
[43] Mason MW, Skedros JG, Bloebaum RD. Evidence of strain-mode-related cortical adaptation in the diaphysis of the horse radius. Bone 1995;17:229–37.
[44] Nalla RK, Kruzic JJ, Kinney JH, Ritchie RO. Mechanistic aspects of fracture and R-curve behavior in human cortical bone. Biomaterials 2005;26:217–31.
[45] Neville AC. Optical methods in cuticle research. In: Miller TA, editor. Cuticle techniques in arthropods. New York, NY: Springer-Verlag; 1980. p. 45–89.
[46] Nunamaker DM, Butterweck DM. Bone modeling and remodeling in the thoroughbred racehorse: Relationships of exercise to bone morphometry. Trans Orthop Res Soc 1989;14:99.
[47] Nyman JS, Roy A, Tyler JH, Acuna RL, Gayle HJ, Wang X. Age-related factors affecting the postyield energy dissipation of human cortical bone. J Orthop Res 2007;25:646–55.
[48] Reilly DT, Burstein AH. The elastic and ultimate properties of compact bone tissue. J Biomech 1975;8:393–405.
[49] Reilly DT, Burstein AH. The mechanical properties of cortical bone. J Bone Joint Surg 1974;56-A:1001–22.
[50] Reilly GC, Currey JD. The effects of damage and microcracking on the impact strength of bone. J Biomech 2000;33:337–43.
[51] Riggs CM, Lanyon LE, Boyde A. Functional associations between collagen fibre orientation and locomotor strain direction in cortical bone of the equine radius. Anat Embryol 1993;187:231–8.
[52] Riggs CM, Vaughan LE, Boyde A, Lanyon LE. Mechanical implications of collagen fibre orientation in cortical bone of the equine radius. Anat Embryol 1993;187: 239–48.
[53] Rubin CT, Lanyon LE. Limb mechanics as a function of speed and gait: A study of functional strains in the radius and tibia of horse and dog. J Exp Biol 1982;101: 187–211.
[54] Rubin CT, McLeod KJ. Biologic modulation of mechanical influences in bone remodeling. In: Mow VC, Ratcliffe A, Woo SL-Y, editors. Biomechanics of diarthrodial joints, 2. New York: Springer-Verlag; 1990. p. 97–118.
[55] Rubin CT, McLeod KJ, Bain SD. Functional strains and cortical bone adaptation: Epigenetic assurance of skeletal integrity. J Biomech 1990;23:43–54.
[56] Schneider RK, Milne DW, Gabel AA, Groom JJ, Bramlage LR. Multidirectional *in vivo* strain analysis of the equine radius and tibia during dynamic loading with and without a cast. Am J Vet Res 1982;43:1541–50.
[57] Skedros JG, Bloebaum RD, Mason MW, Bramble DM. Analysis of a tension/compression skeletal system: possible strain-specific differences in the hierarchical organization of bone. Anat Rec 1994;239:396–404.
[58] Skedros JG, Dayton MR, Sybrowsky CL, Bloebaum RD, Bachus K. The influence of collagen fiber orientation and other histocompositional characteristics on the mechanical properties of equine cortical bone. J Exp Biol 2006;209:3025–42.
[59] Skedros JG, Grunander TR, Hamrick MW. Spatial distribution of osteocyte lacunae in equine radii and third metacarpals: considerations for cellular communication, microdamage detection and metabolism. Cells, Tissues, Organs 2005;180:215–36.
[60] Skedros JG, Holmes JL, Vajda EG, Bloebaum RD. Cement lines of secondary osteons in human bone are not mineral-deficient: new data in a historical perspective. Anat Rec A Discov Mol Cell Evol Biol 2005;286:781–803.
[61] Skedros JG, Hunt KJ. Does the degree of laminarity mediate site-specific differences in collagen fiber orientation in primary bone? An evaluation in the turkey ulna diaphysis. J Anat 2004;205:121–34.

[62] Skedros JG, Hunt KJ, Bloebaum RD. Relationships of loading history and structural and material characteristics of bone: development of the mule deer calcaneus. J Morphol 2004;259:281–307.
[63] Skedros JG, Hunt KJ, Dayton MR, Bloebaum RD, Bachus KN. The influence of collagen fiber orientation on mechanical properties of cortical bone of an artiodactyl calcaneus: Implications for broad applications in bone adaptation. Trans Orthop Res Soc 2003;28:411.
[64] Skedros JG, Kuo TY. Ontogenetic changes in regional collagen fiber orientation suggest a role for variant strain stimuli in cortical bone construction. J Bone Miner Res 1999;14:S441.
[65] Skedros JG, Mason MW, Nelson MC, Bloebaum RD. Evidence of structural and material adaptation to specific strain features in cortical bone. Anat Rec 1996;246: 47–63.
[66] Skedros JG, Sorenson SM, Hunt KJ, Holyoak JD. Ontogenetic structural and material variations in ovine calcanei: a model for interpreting bone adaptation. Anat Rec 2007;290:284–300.
[67] Skedros JG, Sorenson SM, Jenson NH. Are distributions of secondary osteon variants useful for interpreting load history in mammalian bones? Cells Tissues Organs 2007;185:285–307.
[68] Skedros JG, Su SC, Bloebaum RD. Biomechanical implications of mineral content and microstructural variations in cortical bone of horse, elk, and sheep calcanei. Anat Rec 1997;249:297–316.
[69] Sokal RR, Rohlf FJ. Biometry. The Principles and Practice of Statistics in Biological Research. 3rd edition. New York: W.H. Freeman and Co; 1995.
[70] Su SC, Skedros JG, Bachus KN, Bloebaum RD. Loading conditions and cortical bone construction of an artiodactyl calcaneus. J Exp Biol 1999;202(Pt 22):3239–54.
[71] Takano Y, Turner CH, Owan I, Martin RB, Lau ST, Forwood MR, et al. Elastic anisotropy and collagen orientation of osteonal bone are dependent on the mechanical strain distribution. J Orthop Res 1999;17:59–66.
[72] Turner AS, Mills EJ, Gabel AA. *In vivo* measurement of bone strain in the horse. Am J Vet Res 1975;36:1573–9.
[73] Turner CH, Burr DB. Orientation of collagen in osteonal bone. Calcif Tissue Int 1997;60:88–9.
[74] van Oers RF, Ruimerman R, Tanck E, Hilbers PA, Huiskes R. A unified theory for osteonal and hemi-osteonal remodeling. Bone 2008;42:250–9.
[75] van Oers RFM, Ruimerman R, Hilbers PA, Huiskes R. Relating osteon diameter to strain. Pre-ORS (Orthopaedic Research Society) 2006;14th Annual Symposium on Computational Methods in Orthopaedic Biomechanics: *http://www.pre-ors.org/abstracts/preors2006/vanOers_RFM.pdf*.
[76] von Ebner V. Über den feineren bau der skeletteile der kalkschwamme usw. Wiener Stizber 1887;95:213–36.
[77] Wang XD, Masilamani NS, Mabrey JD, Alder ME, Agrawal CM. Changes in the fracture toughness of bone may not be reflected in its mineral density, porosity, and tensile properties. Bone 1998;23:67–72.